The Effect of Phase and Amplitude Imbalance on the Performance of BPSK/QPSK Communication Systems

H. Tsou
Communications Systems and Research Section

The balanced modulator, which is comprised of two matched amplitude-modulation modules, is widely used in phase-modulated communication systems. In practice, the perfect balance between these amplitude-modulation modules is difficult to maintain, and the amplitude and phase imbalance can cause signal distortion and also introduce an undesired interfering tone signal component when such an unbalanced modulator is used to modulate the data directly onto the RF carrier. The rendered imperfection inevitably degrades the receiver performance and, particularly in a quadrature-phase-shift-keyed (QPSK) system, causes cross-talk between channels. This article describes the error performance of binary-phase-shift-keyed (BPSK) and QPSK signals generated from unbalanced modulators and tracked by the conventional Costas loop and a generalized Costas loop, respectively, with the effect of modulator unbalance on the steady-state lock points of these carrier tracking loops being taken into consideration. Also, a more generalized model that includes the possible phase deviation from the ideal 90-deg separation between the in-phase and quadrature channels of QPSK is considered in this article.

I. Introduction

The balanced modulator [1], which is comprised of two matched amplitude-modulation (AM) modules, is widely used to generate suppressed-carrier binary-phase-shift-keyed (BPSK) signals. However, in practice, the perfect balance between these AM modules is difficult to maintain and, when unbalanced modulators are used in missions where the carrier is directly modulated by data without using a subcarrier, the amplitude and phase imbalance not only causes signal distortion but also introduces interfering tone signal components at the carrier frequency. The imperfection rendered from such an unbalanced modulator inevitably degrades the receiver performance and, for the quadrature-phase-shift-keyed (QPSK) system in particular, causes cross-talk between the in-phase (I) and quadrature (Q) channels. In the past, several papers [2–5] studied the effect of such modulator unbalances for Category A missions[1] from different aspects, including the carrier suppression level, power flux density, carrier-tracking performance,

[1] Those missions having an altitude above the Earth of less than 2 million kilometers are treated by the Consultative Committee for Space Data Systems (CCSDS) as Category A missions, and all others belong to Category B. No use of subcarrier is recommended by the CCSDS for missions in Category A; however, it is recommended for Category B missions.

and bit-error performance. Unfortunately, none of these studies recognized the effect of modulator unbalances on the steady-state lock point of the carrier tracking loop, which turns out to be crucial to the determination of accurate bit-error performance. This article addresses this particular issue for the conventional Costas loop for BPSK signals with its error signal formed from an in-phase and quadrature (IQ) product as well as a generalized Costas loop for QPSK signals with its error signal formed from an $\mathrm{IQ}(\mathrm{I}^2 - \mathrm{Q}^2)$ type of product. Furthermore, in addition to the individual phase imbalance existing within the in-phase and quadrature channels of a QPSK system, this article takes the possible phase deviation from the ideal 90-deg separation between channels into consideration, rendering more generalized results.

Section II of this article discusses the effects of an unbalanced modulator on typical QPSK signals, of which the in-phase and quadrature channels are intended to have the same bit rate, denoted as R_b, and equal power, $(P/2)$. Similar effects on BPSK signals can be obtained readily from this same discussion since a BPSK modulator can be regarded as a part of the QPSK modulator, consisting of either of the two channels. The unbalanced modulator effects on the steady-state carrier-tracking lock points of the Costas loops used for carrier tracking are derived in Section III, followed by an evaluation in Section IV of BPSK/QPSK bit-error performance for the combinations of amplitude and phase unbalances within the current Consultative Committee for Space Data Systems' (CCSDS') recommended maximum permissible imbalance figures. By assuming perfect carrier tracking, only the effect on the data detection process is presented there. The combined effects of the modulator imbalance on the data detection process as well as the carrier-tracking process can be numerically realized, with an assumption of Tikhonov distribution for the carrier phase error. Section V concludes this article by providing some remarks and recommendations on maximum permissible imbalance for different performance requirements.

II. Unbalanced BPSK and QPSK Modulators

The QPSK modulator implemented with two balanced modulators, one for the in-phase channel and the other for the quadrature channel, is shown in the block diagram given as Fig. 1. For each channel, the binary, equally probable data of the non-return-to-zero (NRZ) format is fed into two AM modulators, one of them receiving the data stream with inverted polarity. The outputs from these AM modules subtract to form a BPSK signal. With the modulator unbalances, the I-channel and Q-channel signals can be modeled, respectively, by

$$S_{01}(t) = \left(\frac{\sqrt{P}}{2}\right) m_1(t) \left[\cos(\omega_c t + \theta_1) + \Gamma_1 \cos(\omega_c t + \theta_1 + \Delta\theta_1)\right]$$

$$+ \left(\frac{\sqrt{P}}{2}\right) \left[\cos(\omega_c t + \theta_1) - \Gamma_1 \cos(\omega_c t + \theta_1 + \Delta\theta_1)\right] \qquad (1)$$

and

$$S_{02}(t) = \left(\frac{\sqrt{P}}{2}\right) m_2(t) \left[\sin(\omega_c t + \theta_2) + \Gamma_2 \sin(\omega_c t + \theta_2 + \Delta\theta_2)\right]$$

$$+ \left(\frac{\sqrt{P}}{2}\right) \left[\sin(\omega_c t + \theta_2) - \Gamma_2 \sin(\omega_c t + \theta_2 + \Delta\theta_2)\right] \qquad (2)$$

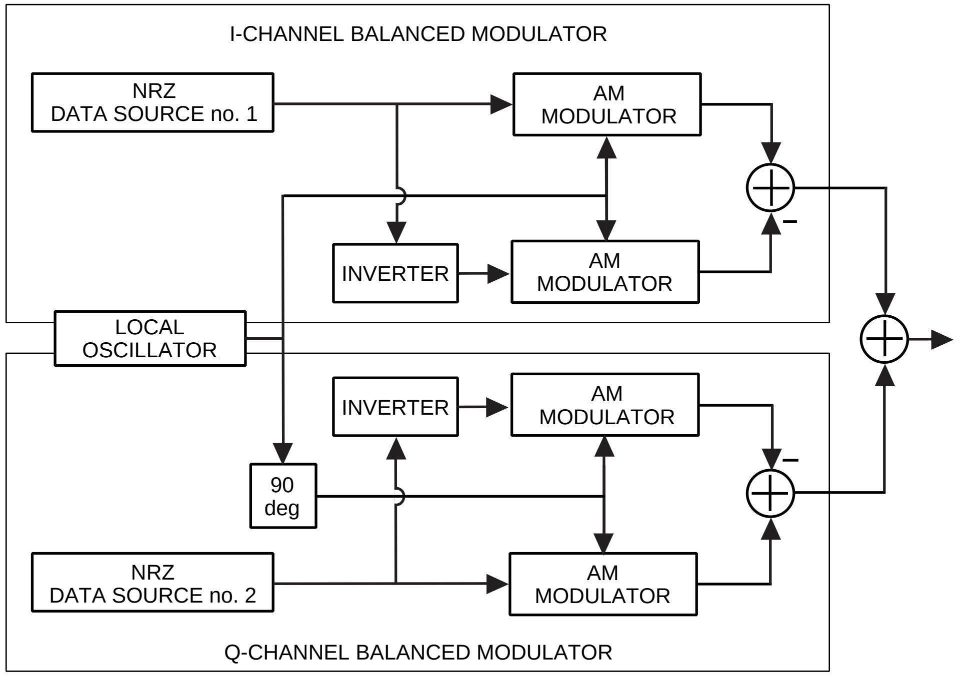

Fig. 1. The QPSK modulator.

where

$m_1(t), m_2(t) =$ the binary data streams for the I-channel and the Q-channel, respectively,

$\theta_1, \theta_2 =$ the local oscillator phases of the I-channel and Q-channel balanced modulators, respectively,

$\Gamma_1, \Gamma_2 =$ the relative amplitude imbalances (assumed to be less than 1) in the I-channel and Q-channel balanced modulators, respectively, and

$\Delta\theta_1, \Delta\theta_2 =$ the phase imbalances between the two AM modulators in the I-channel and Q-channel balanced modulators, respectively.

The resulting QPSK signal, $S_0(t) = S_{01}(t) + S_{02}(t)$, is the combination of the I-channel and Q-channel signals. It is obvious that, in both Eqs. (1) and (2), the first terms are the desired modulated signal components and the second terms are the interfering carrier components, all affected by the modulator unbalances. Moreover, in practice, the phase between the I-channel and Q-channel can deviate from its ideal 90-deg separation, rendering an interchannel phase imbalance denoted as $\Delta\theta = \theta_1 - \theta_2$. Figure 2 shows the phasor representation of the resulting QPSK signal. By assuming $\theta_2 = 0$ without losing the generality, the QPSK signal $S_0(t)$ can be rewritten as

$$S_0(t) = \sqrt{P}\left[(\alpha_1 \cos\omega_c t + \delta_1 \sin\omega_c t) + m_1(t)\left(\beta_1 \cos\omega_c t - \gamma_1 \sin\omega_c t\right)\right]$$

$$+ \sqrt{P}\left[(\alpha_2 \sin\omega_c t - \gamma_2 \cos\omega_c t) + m_2(t)\left(\beta_2 \sin\omega_c t + \gamma_2 \cos\omega_c t\right)\right] \qquad (3)$$

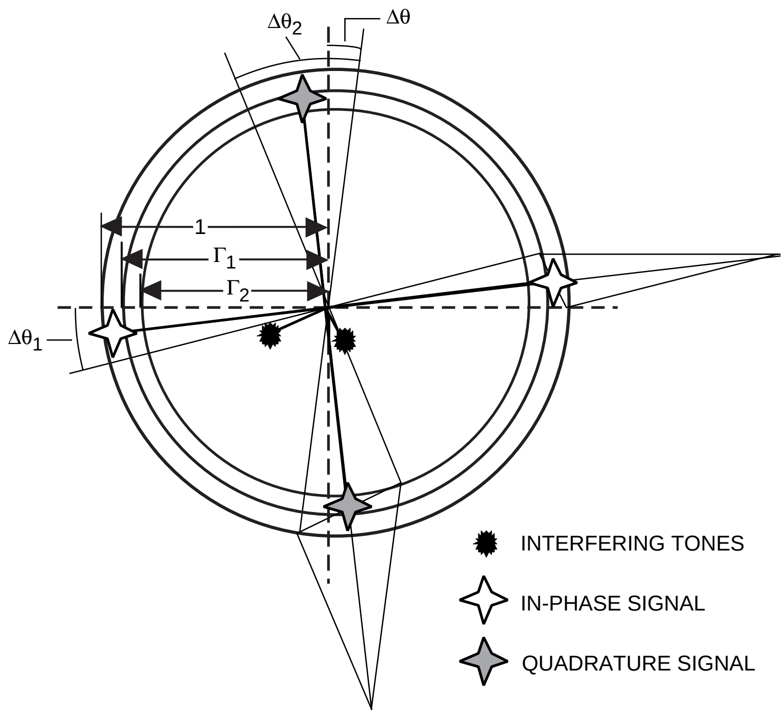

Fig. 2. Phasor representation of the imperfect QPSK signal.

where

$$\alpha_1 = \frac{(1 - \Gamma_1 \cos\Delta\theta_1)\cos\Delta\theta + \Gamma_1 \sin\Delta\theta_1 \sin\Delta\theta}{2}; \quad \alpha_2 = \frac{1 - \Gamma_2 \cos\Delta\theta_2}{2}$$

$$\beta_1 = \frac{(1 + \Gamma_1 \cos\Delta\theta_1)\cos\Delta\theta - \Gamma_1 \sin\Delta\theta_1 \sin\Delta\theta}{2}; \quad \beta_2 = \frac{1 + \Gamma_2 \cos\Delta\theta_2}{2}$$

$$\gamma_1 = \frac{(1 + \Gamma_1 \cos\Delta\theta_1)\sin\Delta\theta + \Gamma_1 \sin\Delta\theta_1 \cos\Delta\theta}{2}; \quad \gamma_2 = \frac{\Gamma_2 \sin\Delta\theta_2}{2}$$

$$\delta_1 = \frac{-(1 - \Gamma_1 \cos\Delta\theta_1)\sin\Delta\theta + \Gamma_1 \sin\Delta\theta_1 \cos\Delta\theta}{2}$$

or, equivalently, as

$$S_0(t) = \sqrt{P}\left\{\left[\alpha_1 + \beta_1 m_1(t) - \gamma_2\left(1 - m_2(t)\right)\right]\cos\omega_c t + \left[\alpha_2 + \beta_2 m_2(t) + \delta_1 - \gamma_1 m_1(t)\right]\sin\omega_c t\right\} \quad (4)$$

in which the cross-talk introduced by the modulator unbalances can be identified easily.

For the case of $\Delta\theta_1 = \Delta\theta_2 = \Delta\theta = 0$, it can easily be verified that the cross-talk disappears from the modulated signal even though the amplitude imbalance still exists. However, it is important to know that the lack of cross-talk in modulated signals does not guarantee the absence of cross-talk on the receiver side. Actually, in this special case, cross-talk may still exist due to imperfect carrier tracking resulting from the amplitude imbalance in the unbalanced QPSK modulator.

The BPSK signal is readily realized as the Q-channel signal $S_{02}(t)$ given in Eq. (2) and can be expressed in exactly the same form as the second term of Eq. (3) or, equivalently, in the form of Eq. (4) with $\alpha_1 = \beta_1 = \gamma_1 = \delta_1 = 0$.

III. Steady-State Lock Point of the Carrier-Tracking Loop

For the conventional Costas loop used to track the suppressed carrier of BPSK signals [see Fig. 3(a)], the received signal first is mixed with the I-arm and Q-arm reference signals, e.g., $\sqrt{2}\cos(\omega_c t - \phi)$ and $\sqrt{2}\sin(\omega_c t - \phi)$, and then passed through the integrate-and-dump (I&D) filters on both arms of the Costas loop, which are assumed to be driven by a perfectly synchronized symbol clock, rendering

$$\left.\begin{aligned} V_1 &= \sqrt{\frac{P}{2}}\left(\frac{1}{R_b}\right)\left[(\alpha_2 + \beta_2 d_0)\cos\phi + \gamma_2(1 - d_0)\sin\phi\right] \\ V_2 &= \sqrt{\frac{P}{2}}\left(\frac{1}{R_b}\right)\left[(\alpha_2 + \beta_2 d_0)\sin\phi - \gamma_2(1 - d_0)\cos\phi\right] \end{aligned}\right\} \tag{5}$$

where d_0 is a data bit taking ± 1 with equal probability. The error signal for loop feedback, denoted as z_0, is then formed as a product of V_1 and V_2. Carrying out the average over d_0 and equating the averaged error signal, denoted as $\overline{z_0}$, to 0, one can solve for the steady-state lock point, denoted as ϕ_0, of the Costas loop. It turns out that

$$\phi_0 = -\frac{1}{2}\tan^{-1}\left(\frac{\Gamma^2 \sin(2\Delta\theta)}{1 + \Gamma^2\cos(2\Delta\theta)}\right) \tag{6}$$

where Γ and $\Delta\theta$ are the amplitude and phase imbalance from the unbalanced BPSK modulator, respectively. Note that for $\Gamma = 1$, $\phi_0 = -\Delta\theta/2$ as expected.

For the generalized Costas loop used to track the suppressed carrier of QPSK signals [see Fig. 3(b)], everything remains the same except that the error signal is now formed from an $\mathrm{IQ}(\mathrm{I}^2 - \mathrm{Q}^2)$ type of product, with I and Q being the output variables V_1 and V_2 from the I&D filters on the corresponding arms of the generalized Costas loop. It can be shown that

$$\left.\begin{aligned} V_1 &= \sqrt{\frac{P}{2}}\left(\frac{1}{R_b}\right)\left[(\alpha_1 + \beta_1 a_0 - \gamma_2(1 - b_0))\cos\phi + (\alpha_2 + \beta_2 b_0 + \delta_1 - \gamma_1 d_0)\sin\phi\right] \\ V_2 &= \sqrt{\frac{P}{2}}\left(\frac{1}{R_b}\right)\left[-(\alpha_1 + \beta_1 a_0 - \gamma_2(1 - b_0))\sin\phi + (\alpha_2 + \beta_2 b_0 + \delta_1 - \gamma_1 d_0)\cos\phi\right] \end{aligned}\right\} \tag{7}$$

where a_0 and b_0 are data bits from the in-phase and quadrature data streams, each taking ± 1 with equal probability. The steady-state lock point of the generalized Costas loop can be found in the same way as that described previously for the Costas loop, namely, by carrying out the average over a_0 and b_0 and equating $\overline{z_0}$ to 0. However, the close-form solution of such a generalized Costas loop is very messy, involving all five arguments (i.e., $\Gamma_1, \Gamma_2, \Delta\theta_1, \Delta\theta_2$, and $\Delta\theta$), and can be solved only numerically. Nevertheless, it is still interesting to find that for a special case of identically unbalanced in-phase and quadrature modulators with perfect 90-deg separation between these channels, namely

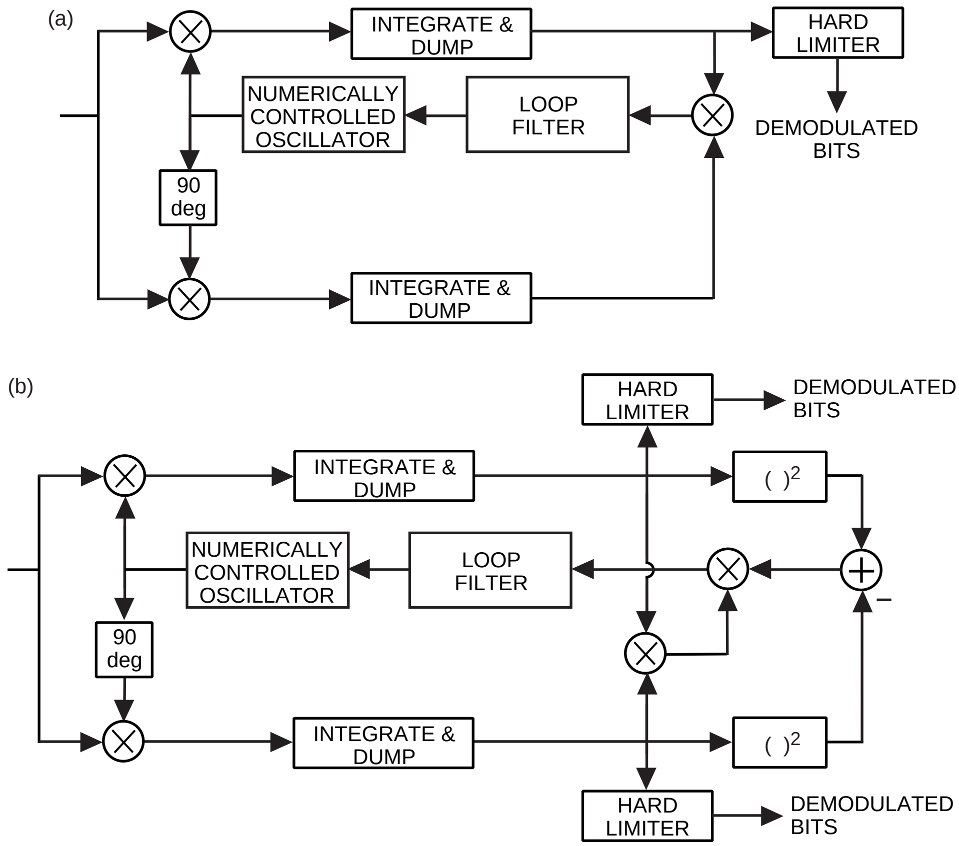

Fig. 3. Costas loops: (a) conventional loop for BPSK signals and (b) generalized loop for QPSK signals.

$$\Gamma_1 = \Gamma_2 = \Gamma$$

$$\Delta\theta_1 = \Delta\theta_2 = \Delta\theta_u$$

and

$$\Delta\theta = 0$$

a simple close form of ϕ_0 does exist as

$$\phi_0 = -\frac{1}{4}\tan^{-1}\left(\frac{6\Gamma^2\sin(2\Delta\theta_u) + \Gamma^4\sin(4\Delta\theta_u)}{1 + 6\Gamma^2\cos(2\Delta\theta_u) + \Gamma^4\cos(4\Delta\theta_u)}\right) \tag{8}$$

Note that for $\Gamma = 1$, one has $\phi_0 = -\Delta\theta_u/2$ as expected.

IV. Bit-Error Performance

The error performance is determined by the average bit-error probability associated with the demodulated data stream(s). It can be calculated by first finding the conditional (on the carrier phase error) bit-error probability, $P_b(\phi)$, for a given carrier phase error, ϕ, and then taking the average over the probability density function of the phase error, denoted as $P(\phi)$, as characterized by the carrier tracking loop.

For BPSK signals, making a hard decision on V_1 in Eq. (5) produces the decision on the bit d_0. It is straightforward to show that, when the transmitted signal is corrupted by additive white Gaussian noise with two-sided power spectral density $N_0/2$ W/Hz, the conditional bit-error probability associated with this decision is

$$P_b(\phi) = \frac{1}{4}\,\text{erfc}\left(\sqrt{\frac{E_b}{N_0}}\cos\phi\right) + \frac{1}{4}\,\text{erfc}\left(\sqrt{\frac{E_b}{N_0}}\Gamma\cos(\phi - \Delta\theta)\right) \tag{9}$$

where $E_b = P/R_b$ is the bit energy. For the conventional Costas loop operated at an infinity loop SNR, the carrier phase error will remain as ϕ_0 with probability 1 and, therefore, the average bit-error probability for such a perfectly synchronized carrier becomes $P_b(\phi_0)$. Figure 4 is a plot of the average bit-error probability, with perfect carrier synchronization assumed, as a function of E_b/N_0 for the best and the worst combinations within the range constrained by the maximum amplitude imbalance of 0.2 dB and the maximum phase imbalance of 2 deg recommended by the CCSDS. For realistic scenarios with imperfect carrier tracking, a Tikhonov distribution of carrier-tracking phase error centered at ϕ_0 is assumed. The average bit-error probability can be evaluated by further assuming that the 180-deg phase ambiguity can be perfectly resolved as

$$P_b = \int_{\phi_0-(\pi/2)}^{\phi_0+(\pi/2)} P_b(\phi)\frac{\exp\left(\rho_{2\phi}\cos(2(\phi-\phi_0))\right)}{\pi I_0(\rho_{2\phi})}d\phi \tag{10}$$

For QPSK signals, making hard decisions on V_1 and V_2 in Eq. (7) produces the decisions on the bits a_0 and b_0, respectively. The conditional bit-error probabilities associated with these decisions are given by

$$\begin{aligned}
P_{b,1}(\phi) = {} & \frac{1}{8}\,\text{erfc}\left(\sqrt{\frac{E_b}{N_0}}\left[\cos(\phi+\Delta\theta)+\sin\phi\right]\right) \\
& + \frac{1}{8}\,\text{erfc}\left(\sqrt{\frac{E_b}{N_0}}\left[\cos(\phi+\Delta\theta)-\Gamma_2\sin\left(\phi+\Delta\theta_2\right)\right]\right) \\
& + \frac{1}{8}\,\text{erfc}\left(\sqrt{\frac{E_b}{N_0}}\left[\Gamma_1\cos\left(\phi+\Delta\theta_1+\Delta\theta\right)-\sin\phi\right]\right) \\
& + \frac{1}{8}\,\text{erfc}\left(\sqrt{\frac{E_b}{N_0}}\left[\Gamma_1\cos\left(\phi+\Delta\theta_1+\Delta\theta\right)+\Gamma_2\sin\left(\phi+\Delta\theta_2\right)\right]\right)
\end{aligned} \tag{11a}$$

and

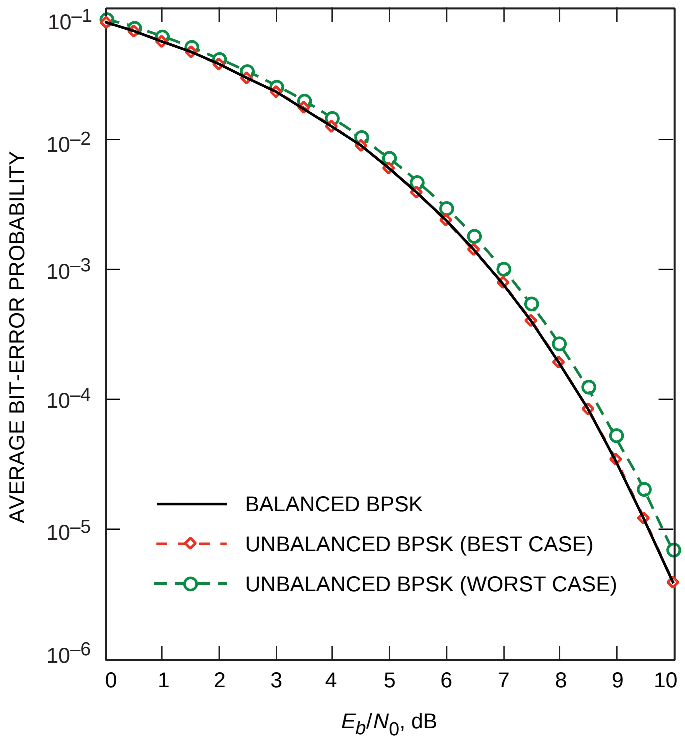

Fig. 4. Bit-error performance of unbalanced BPSK signals.

$$P_{b,2}(\phi) = \frac{1}{8}\,\mathrm{erfc}\left(\sqrt{\frac{E_b}{N_0}}\left[\cos\phi - \sin(\phi + \Delta\theta)\right]\right)$$

$$+\,\frac{1}{8}\,\mathrm{erfc}\left(\sqrt{\frac{E_b}{N_0}}\left[\cos\phi + \Gamma_1 \sin(\phi + \Delta\theta_1 + \Delta\theta)\right]\right)$$

$$+\,\frac{1}{8}\,\mathrm{erfc}\left(\sqrt{\frac{E_b}{N_0}}\left[\Gamma_2 \cos(\phi + \Delta\theta_2) + \sin(\phi + \Delta\theta)\right]\right)$$

$$+\,\frac{1}{8}\,\mathrm{erfc}\left(\sqrt{\frac{E_b}{N_0}}\left[\Gamma_2 \cos\left(\phi + \Delta\theta_2\right) - \Gamma_1 \sin\left(\phi + \Delta\theta_1 + \Delta\theta\right)\right]\right) \qquad \text{(11b)}$$

where $P_{b,1}(\phi)$ and $P_{b,2}(\phi)$ are associated with the in-phase and quadrature channels, respectively. Note that the error performances of these two channels are, in general, not identical under modulator unbalances. The average bit-error probability for QPSK signals is the arithmetic average of Eqs. (11a) and (11b), given that both channels have the same power and bit rate.

By substituting ϕ_0 found for the generalized QPSK Costas loop into Eqs. (11a) and (11b), the average QPSK bit-error probability and the individual bit-error probabilities for both channels can be evaluated as a function of E_b/N_0 for the perfect carrier synchronization case. Table 1 lists these probabilities

Table 1. QPSK bit-error performance under various combinations of modulator unbalances.

$\Delta\theta$, deg	Γ_1, dB	$\Delta\theta_1$, deg	Γ_2, dB	$\Delta\theta_2$, deg	$P_{b,Avg}$ at $E_b/N_0 = 10$ dB	$P_{b,I}$ at $E_b/N_0 = 10$ dB	$P_{b,Q}$ at $E_b/N_0 = 10$ dB	ϕ_0, deg	Remarks
0	0	0	0	0	3.8721×10^{-6}	3.8721×10^{-6}	3.8721×10^{-6}	0.0000	Ideal case
0	−0.2	2	−0.2	2	7.2178×10^{-6}	6.2257×10^{-6}	8.2099×10^{-6}	−0.9770	
0	−0.2	2	0	2	5.1716×10^{-6}	6.2204×10^{-6}	4.1228×10^{-6}	−0.9880	
0	0	2	−0.2	2	6.1876×10^{-6}	4.1226×10^{-6}	8.2527×10^{-6}	−0.9869	(3)
0	0	2	0	2	4.1340×10^{-6}	4.1340×10^{-6}	4.1340×10^{-6}	−1.0000	(1), (2)
0	−0.2	2	−0.2	−2	8.6599×10^{-6}	8.6599×10^{-6}	8.6599×10^{-6}	0.0000	(2)
0	−0.2	2	0	−2	6.5835×10^{-6}	8.7977×10^{-6}	4.3692×10^{-6}	−0.0076	(3)
0	0	2	−0.2	−2	6.5835×10^{-6}	4.3692×10^{-6}	8.7977×10^{-6}	0.0076	(3)
0	0	2	0	−2	4.4196×10^{-6}	4.4196×10^{-6}	4.4196×10^{-6}	0.0000	(2)
0	−0.2	−2	−0.2	2	6.6031×10^{-6}	6.6031×10^{-6}	6.6031×10^{-6}	0.0000	(2)
0	−0.2	−2	0	2	5.4917×10^{-6}	6.6336×10^{-6}	4.3499×10^{-6}	0.0111	
0	0	−2	−0.2	2	5.4917×10^{-6}	4.3499×10^{-6}	6.6336×10^{-6}	−0.0111	
0	0	−2	0	2	4.4011×10^{-6}	4.4011×10^{-6}	4.4011×10^{-6}	0.0000	(2)
0	−0.2	−2	−0.2	−2	7.2178×10^{-6}	8.2099×10^{-6}	6.2257×10^{-6}	0.9770	
0	−0.2	−2	0	−2	6.1876×10^{-6}	8.2527×10^{-6}	4.1226×10^{-6}	0.9869	
0	0	−2	−0.2	−2	5.1716×10^{-6}	4.1228×10^{-6}	6.2204×10^{-6}	0.9880	
0	0	−2	0	−2	4.1340×10^{-6}	4.1340×10^{-6}	4.1340×10^{-6}	1.0000	(1), (2)
2	−0.2	2	−0.2	2	7.6125×10^{-6}	6.6109×10^{-6}	8.6141×10^{-6}	−1.9793	
2	−0.2	2	0	2	5.4917×10^{-6}	6.6336×10^{-6}	4.3499×10^{-6}	−2.0112	
2	0	2	−0.2	2	6.5714×10^{-6}	4.3841×10^{-6}	8.7587×10^{-6}	−1.9661	(3)
2	0	2	0	2	4.4011×10^{-6}	4.4011×10^{-6}	4.4011×10^{-6}	−2.0000	(2)
2	−0.2	2	−0.2	−2	1.0124×10^{-5}	1.0124×10^{-5}	1.0124×10^{-5}	−1.0000	(2)
2	−0.2	2	0	−2	7.8099×10^{-6}	1.0466×10^{-5}	5.1544×10^{-6}	−1.0280	(3)
2	0	2	−0.2	−2	7.8099×10^{-6}	5.1544×10^{-6}	1.0466×10^{-5}	−0.9720	(3)
2	0	2	0	−2	5.2971×10^{-6}	5.2971×10^{-6}	5.2971×10^{-6}	−1.0000	(2)
2	−0.2	−2	−0.2	2	6.2256×10^{-6}	6.2256×10^{-6}	6.2256×10^{-6}	−1.0000	(2)
2	−0.2	−2	0	2	5.1716×10^{-6}	6.2204×10^{-6}	4.1228×10^{-6}	−1.0120	
2	0	−2	−0.2	2	5.1716×10^{-6}	4.1228×10^{-6}	6.2204×10^{-6}	−0.9880	
2	0	−2	0	2	4.1340×10^{-6}	4.1340×10^{-6}	4.1340×10^{-6}	−1.0000	(1), (2)
2	−0.2	−2	−0.2	−2	7.6125×10^{-6}	8.6141×10^{-6}	6.6109×10^{-6}	−0.0207	
2	−0.2	−2	0	−2	6.5714×10^{-6}	8.7587×10^{-6}	4.3841×10^{-6}	−0.0339	(3)
2	0	−2	−0.2	−2	5.4917×10^{-6}	4.3499×10^{-6}	6.6336×10^{-6}	0.0111	
2	0	−2	0	−2	4.4011×10^{-6}	4.4011×10^{-6}	4.4011×10^{-6}	0.0000	(2)
−2	−0.2	2	−0.2	2	7.6909×10^{-6}	6.6138×10^{-6}	8.7680×10^{-6}	0.0255	
−2	−0.2	2	0	2	5.5242×10^{-6}	6.6457×10^{-6}	4.4026×10^{-6}	0.0351	
−2	0	2	−0.2	2	6.5835×10^{-6}	4.3692×10^{-6}	8.7977×10^{-6}	−0.0076	(3)
−2	0	2	0	2	4.4196×10^{-6}	4.4196×10^{-6}	4.4196×10^{-6}	0.0000	(2)
−2	−0.2	2	−0.2	−2	8.2104×10^{-6}	8.2104×10^{-6}	8.2104×10^{-6}	1.0000	(2)
−2	−0.2	2	0	−2	6.1876×10^{-6}	8.2527×10^{-6}	4.1226×10^{-6}	1.0131	(3)
−2	0	2	−0.2	−2	6.1876×10^{-6}	4.1226×10^{-6}	8.2527×10^{-6}	0.9869	(3)
−2	0	2	0	−2	4.1340×10^{-6}	4.1340×10^{-6}	4.1340×10^{-6}	1.0000	(1), (2)
−2	−0.2	−2	−0.2	2	7.7996×10^{-6}	7.7996×10^{-6}	7.7996×10^{-6}	1.0000	(2)
−2	−0.2	−2	0	2	6.5236×10^{-6}	7.9385×10^{-6}	5.1087×10^{-6}	1.0339	
−2	0	−2	−0.2	2	6.5236×10^{-6}	5.1087×10^{-6}	7.9385×10^{-6}	0.9661	
−2	0	−2	0	2	5.2540×10^{-6}	5.2540×10^{-6}	5.2540×10^{-6}	1.0000	(2)
−2	−0.2	−2	−0.2	−2	7.6909×10^{-6}	8.7680×10^{-6}	6.6138×10^{-6}	1.9745	
−2	−0.2	−2	0	−2	6.5835×10^{-6}	8.7977×10^{-6}	4.3692×10^{-6}	2.0076	(3)
−2	0	−2	−0.2	−2	5.5242×10^{-6}	4.4026×10^{-6}	6.6457×10^{-6}	1.9649	
−2	0	−2	0	−2	4.4196×10^{-6}	4.4196×10^{-6}	4.4196×10^{-6}	2.0000	(2)

(1) Orthogonal signal constellation.
(2) Balanced in-phase and quadrature-phase performance.
(3) Highly unbalanced in-phase and quadrature-phase performance.

at an E_b/N_0 of 10 dB for all the possible combinations within the range constrained by the maximum amplitude imbalance of 0.2 dB, the maximum phase imbalance of 2 deg recommended by the CCSDS, and the maximum interchannel phase imbalance of 2 deg. It is interesting to note that performance degradation exists in all of the cases evaluated here, even if the signal constellation is orthogonal and the steady-state lock point of the tracking loop is correctly located, e.g., those four cases having both (1) and (2) in the remarks column of Table 1. The cause of a small degradation in these four cases is from their interfering carrier components. Also, both highly unbalanced and balanced bit-error performances among those two channels can be identified for certain combinations from this table, giving an indication of how different these channels can be under the modulator unbalances. Another interesting conclusion that can be made from this table is that the worst combination of modulator unbalances tends to happen when the amplitude imbalance is at its maximum and the phase imbalance for the in-phase and quadrature channels makes them rotate toward each other on a signal phasor diagram, which agrees well with one's intuition. The best and the worst combinations for these bit-error probabilities as functions of E_b/N_0 are plotted in Figs. 5 through 7. For realistic scenarios with imperfect carrier tracking, a Tikhonov distribution of carrier-tracking phase error centered at ϕ_0 is assumed. The average bit-error probability can be evaluated by further assuming that the 90-deg phase ambiguity can be perfectly resolved as

$$P_{b,1} = 2 \int_{\phi_0 - (\pi/4)}^{\phi_0 + (\pi/4)} P_{b,1}(\phi) \frac{\exp\left(\rho_{4\phi} \cos(4(\phi - \phi_0))\right)}{\pi I_0\left(\rho_{4\phi}\right)} d\phi \tag{12a}$$

and

$$P_{b,2} = 2 \int_{\phi_0 - (\pi/4)}^{\phi_0 + (\pi/4)} P_{b,2}(\phi) \frac{\exp\left(\rho_{4\phi} \cos(4(\phi - \phi_0))\right)}{\pi I_0\left(\rho_{4\phi}\right)} d\phi \tag{12b}$$

where $P_{b,1}$ and $P_{b,2}$ are associated with the I-channel and the Q-channel, respectively.

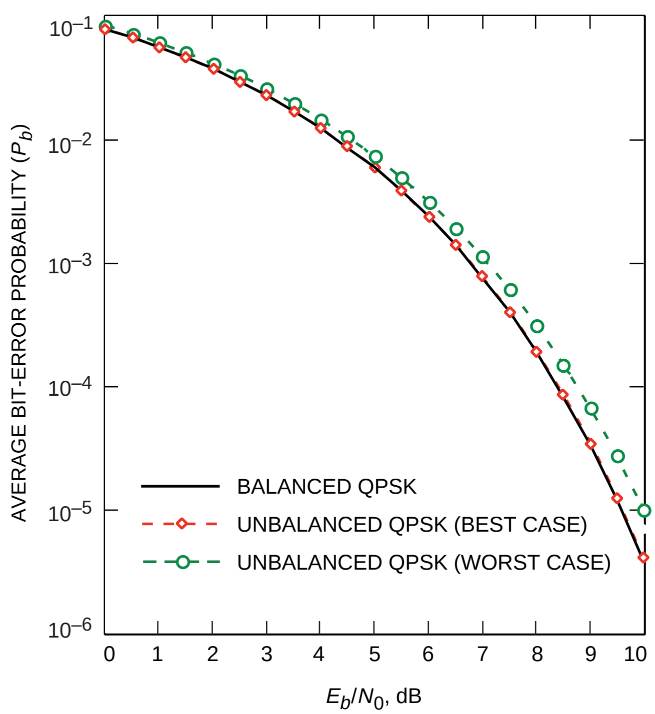

Fig. 5. Bit-error performance of unbalanced QPSK signals.

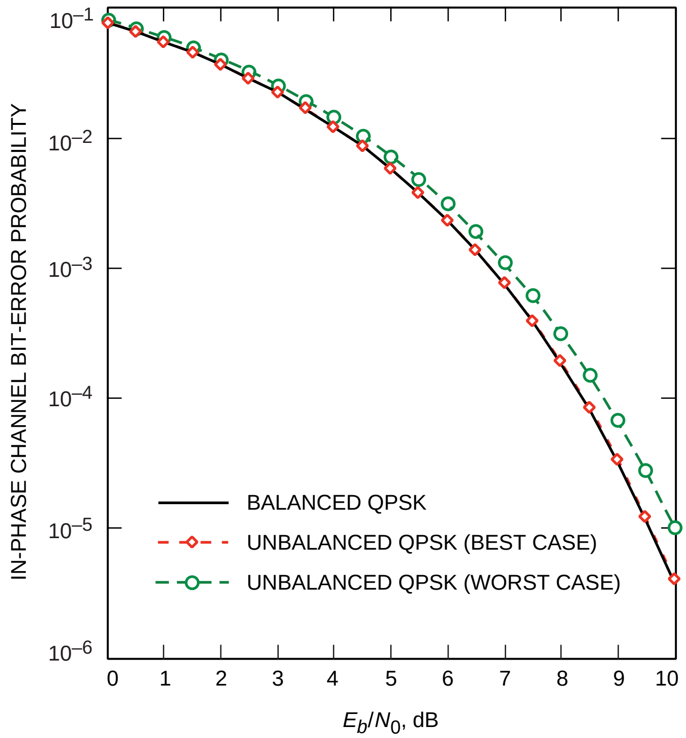

Fig. 6. Bit-error performance of unbalanced QPSK signals: in-phase channel.

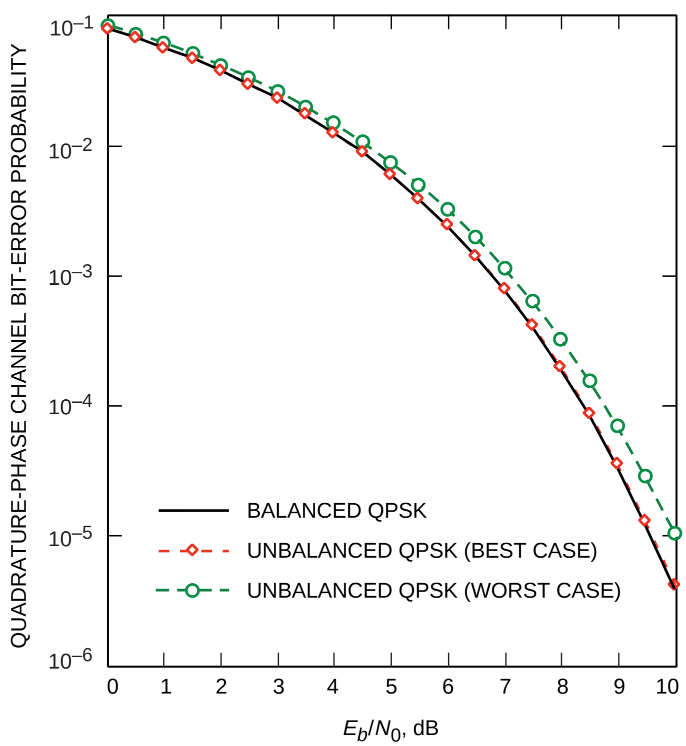

Fig. 7. Bit-error performance of unbalanced QPSK signals: quadrature channel.

V. Conclusions

In this article, the effects of modulator unbalance on the steady-state lock points of the conventional Costas loop and a generalized Costas loop for BPSK and QPSK signals, respectively, were discussed. With the correct lock points derived, the error performances of BPSK and QPSK signals generated by unbalanced modulators and tracked by the corresponding Costas loops were given. For the case of perfect carrier tracking, the bit-error probabilities were evaluated for the combinations of modulator unbalances within the current recommended maximum permissible imbalance figures. The results, which reflect a more general model with possible interchannel phase imbalance between the QPSK channels being considered, were summarized in a table for ease of comparison. It is further noted here that, with the CCSDS recently considering elimination of the use of subcarrier in favor of efficient bandwidth utilization, the results presented in this article can be directly applied to future Category B missions in which no subcarrier is used.

From Figs. 4 through 7, we can see a 0.23-dB and 0.33-dB E_b/N_0 degradation for the worst-case unbalanced BPSK and QPSK signals (overall or individual channels), respectively, at a bit-error rate (BER) of 10^{-2}, under the assumption of perfect carrier synchronization and based upon the current CCSDS recommendations for a 2-deg maximum permissible phase imbalance (including the interchannel phase imbalance for QPSK) and a 0.2-dB amplitude imbalance. The actual performance will be even worse when imperfect carrier tracking is considered.

In order to reduce the degradation to 0.1 dB for unbalanced BPSK signals at a BER of 10^{-2}, as specified for Category B missions in a draft CCSDS recommendation,[2] the maximum permissible phase imbalance has to be reduced to 1 deg and the maximum permissible amplitude imbalance has to be lowered to 0.1 dB, which again is under an assumption of perfect carrier synchronization. More stringent modulator unbalances, such as the maximum permissible phase imbalance (including the interchannel phase imbalance) at 0.75 deg and the maximum permissible amplitude imbalance at 0.08 dB, are required to cut down the degradation for QPSK signals to 0.1 dB under the same perfect carrier synchronization assumption. On the contrary, for unbalanced BPSK signals, the maximum permissible phase imbalance is allowed to increase to 3 deg, and the maximum permissible amplitude imbalance can be raised to 0.25 dB for a 0.4-dB degradation at a BER of 10^{-2}, as specified for Category A missions in the same draft recommendation. For this amount of degradation, the maximum permissible phase imbalance (including the interchannel phase imbalance) should be at 2 deg and the maximum permissible amplitude imbalance at 0.2 dB for unbalanced QPSK signals.

References

[1] B. A. Carlson, *Communication Systems*, 2nd ed., New York: McGraw-Hill, 1975.

[2] J.-L. Gerner, "A Position Paper on the Effect of Phase Unbalanced Modulator on the Performance of PSK Modulation Schemes for Category A Missions," Consultative Committee for Space Data Systems, *Proceedings of the CCSDS RF and Modulation Subpanel 1E Meeting*, CCSDS 421.0-G-1, Green Book, pp. 287–301, September 1989.

[3] T. M. Nguyen and Y. Owens, "Cross-Talk in QPSK Communication Systems," Consultative Committee for Space Data Systems, *Proceedings of the CCSDS RF and Modulation Subpanel 1E Meeting*, CCSDS B20.0-Y-1, Yellow Book, pp. 85–93, September 1993.

[2] This draft recommendation resulted from a study for the CCSDS RF and Modulation Subpanel 1E action item A-E-93-34.

[4] T. M. Nguyen and A. Anabtawi, "Cross-Talk Due to Phase Imbalance Between the Channels in QPSK Communication Systems," presented at the Consultative Committee for Space Data Systems RF and Modulation Subpanel 1E Meeting, Pasadena, California, June 1994.

[5] M. K. Simon, "The Effect of Modulator Unbalance on QPSK Performance," presented at the Consultative Committee for Space Data Systems RF and Modulation Subpanel 1E Meeting, Pasadena, California, May 1996.